ELSEVIER

Wave Motion 35 (2002) 339–353

WAVE MOTION

www.elsevier.com/locate/wavemoti

Propagation of small waves in inextensible strings

Martin Schagerl*, Arno Berger

Institute of Mechanics, Vienna University of Technology, A-1040 Vienna, Austria

Received 29 September 2000; received in revised form 22 May 2001; accepted 18 June 2001

Abstract

The model of an inextensible uniform string subject to constant gravitation is used to study the propagation of transversal waves in one-dimensional continua. Perturbation analysis of the equations of motion yields as a result the local representation of small waves in terms of a normalized Riemann function. By means of the latter, shape and speed of propagating waves may be discussed. A refined analysis confirms that on first order, small waves travel along characteristics of the unperturbed equilibrium configuration. An explicit power law for the waves' amplitudes is given, and the findings are supported by the numerical results.

1. Introduction

One-dimensional continuum models of strings have repeatedly gained importance as basic tools for engineering applications. As a recent application, we mention the usage of various string models in the dynamical analysis of *tethered satellite systems* [2]. When dealing with extensible strings one typically observes both longitudinal and transversal waves [10]. The dynamics of longitudinal waves, however, is regarded as being of minor importance in many cases. For example, tethers between satellites usually are rather stiff thus giving rise to longitudinal waves of very small amplitude. Furthermore, these waves typically propagate extremely fast which generally makes their numerical treatment quite delicate [8]. Moreover, it is well known that the characteristic properties of longitudinal waves heavily depend on the underlying constitutive law, while this is not the case for transversal waves [11]. Focussing on transversal waves may therefore be endorsed for numerical as well as conceptual reasons.

Obviously, the simplest way of ruling out the longitudinal waves is by considering inextensible strings. When discretizing their equations of motion, one is naturally led to the model of a chain of rigid bodies linked by frictionless hinges [9]. Despite its simplicity, the chain model accurately reflects a lot of effects exhibited by the inextensible string. For example, the following experiment may easily be given numerical support: holding the chain's end in one hand and perturbing the vertical equilibrium position by tapping the middle of the chain with one finger of the other hand, one clearly observes two propagating waves (see Fig. 1; we encourage the reader to effectively carry out this experiment). The wave approaching the free end may easily be studied due to its decreasing velocity and increasing amplitude. (This last effect is the more noticeable when the smaller mass is attached at the free end.) The wave propagating towards the upper end of the chain is not as easily observed because it moves increasingly faster and, at the same time, its amplitude decreases.

* Corresponding author. Tel.: +43-1-58801-32556.
E-mail address: martin.schagerl@tuwien.ac.at (M. Schagerl).

0165-2125/02/$ – see front matter
PII: S0165-2125(01)00112-3

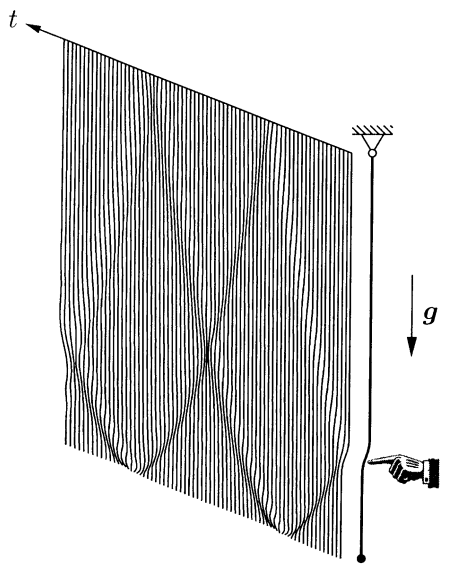

Fig. 1. Travelling waves in the inextensible string pendulum as exhibited by the discrete chain model (320 links; the attached endmass amounts $\frac{1}{21}$ of the total mass).

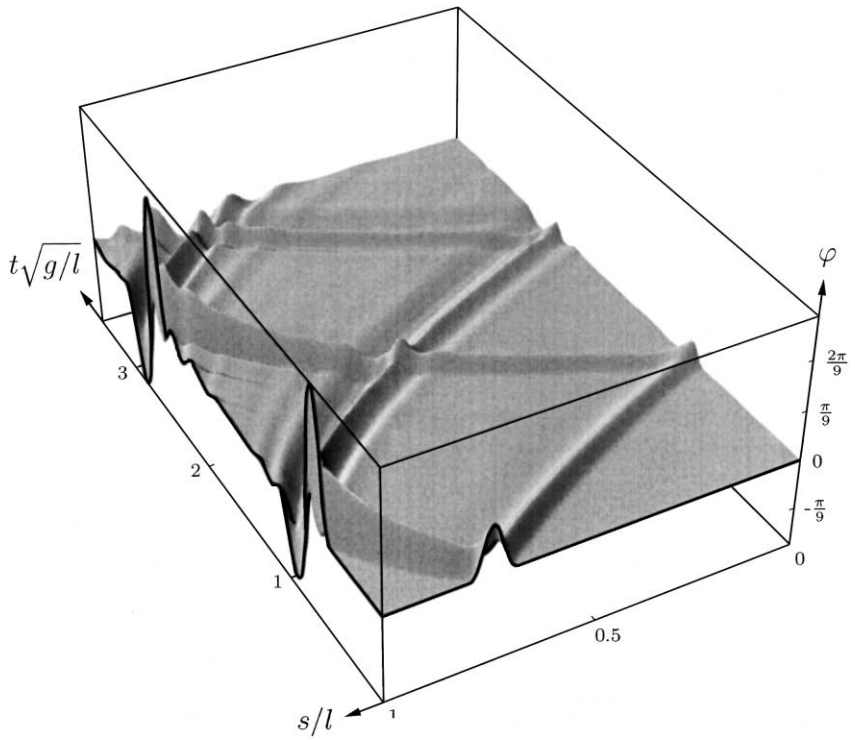

Fig. 2. Angles of the local tangent during the propagation of a small perturbation.

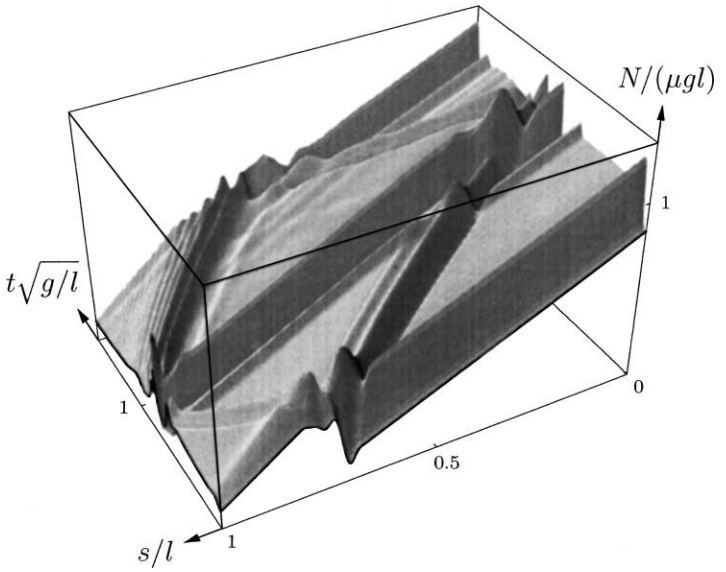

Fig. 3. The string pendulum's tension during the propagation of a small perturbation.

These effects may be made more visible by plotting the angles φ of the chain links. Fig. 2 clearly exhibits the specific evolution of amplitudes mentioned above. Moreover, a projection of the surface in Fig. 2 lucidly shows the propagation of two distinct waves: Light (dark) regions of Fig. 5 correspond to large (small) values of φ. Additionally, the reflections at the ends can be seen very clearly.

From the solution for the angles, the evolution of the axial forces N in the chain links may also be calculated (see Fig. 3 or [7,9]). For the (vertical) equilibrium position, N clearly is linear. As can be seen from Fig. 3, the tension can be considered piecewise linear with high accuracy during the whole propagation process of a small perturbation. Large oscillations in amplitude exclusively occur at reflection times while small oscillations may be observed at crossings of the two waves. The small initial fluctuation is due to the fact that the conditions of equilibrium are not met by the initial data.

As indicated above, the chain model may be used to quickly gain some insight into the dynamics of a string pendulum. Moreover, its numerical treatment does not pose serious problems. When falling back on the continuum model there are, however, some interesting questions implicitly mentioned above which deserve an analysis in their own right: How do the form and amplitude of waves evolve under propagation? Where do the oscillations of the tension come from? How about the reflected waves? The aim of the present paper as well as its sequel [7] is to rigorously deal with these questions by means of perturbation analysis and explicit local representations of solutions for the string's governing equations.

2. Equations of motion

We consider an inextensible string and denote by s the arc-length with respect to an arbitrary reference point fixed on the string (Fig. 4). At time t, the material point with coordinate s finds itself at $\boldsymbol{r}(s,t)$ in the Euclidean $\mathbb{E}^3$. Due to inextensibility, we have

$$\boldsymbol{r}_s(s,t)\cdot\boldsymbol{r}_s(s,t)=1, \tag{1}$$

i.e. $\boldsymbol{r}_s(s,t)$ is a unit vector tangent to the string's configuration. Assuming perfect flexibility for the string (which just says that the contact torque vanishes identically), we observe that the shear component of the contact force $\boldsymbol{n}$

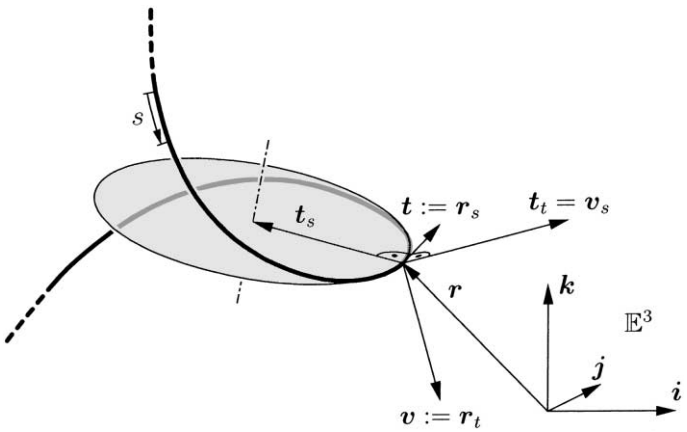

Fig. 4. Inextensible string kinematics at time t.

vanishes (this is an immediate consequence of the balance of angular momentum, cf. [1]); therefore, $\boldsymbol{n}$ necessarily is a multiple of $\boldsymbol{r}_s(s,t)$, i.e.

$$\boldsymbol{n}(s,t) = N(s,t)\,\boldsymbol{r}_s(s,t). \tag{2}$$

Assuming smooth configurations (i.e. no kinks), we deduce the classical form of the equation of motion with respect to an inertial frame,

$$\mu \boldsymbol{r}_{tt}(s,t) = \boldsymbol{n}_s(s,t) + \mu \boldsymbol{g} \quad \text{where} \quad (s,t) \in (-\infty,\infty) \times (0,\infty) \tag{3}$$

by means of the balance of linear momentum [1]. The partial differential equation (3) governs the dynamics of a string with constant mass μ per unit length subject to the stationary and homogenous gravitational field $\boldsymbol{g}$. While (2) and (3) analogously hold for extensible strings, a significant difference should be taken notice of: in the extensible case, tension and deformation are directly linked via constitutive laws. For inextensible strings, however, these laws reduce to the kinematic constraint (1); the tension N may then be interpreted as a Lagrange multiplier within a variational approach from which the equation of motion could equally be derived [3].

After imposing initial values on configuration and velocity,

$$\boldsymbol{r}(s,0) = \bar{\boldsymbol{r}}(s) \quad \text{and} \quad \boldsymbol{r}_t(s,0) = \bar{\boldsymbol{v}}(s), \tag{4}$$

solutions of (2) and (3) may be looked for. Clearly, compatibility with (1) has to be maintained. For the initial conditions, therefore

$$\bar{\boldsymbol{r}}'(s) \cdot \bar{\boldsymbol{r}}'(s) = 1 \quad \text{as well as} \quad \bar{\boldsymbol{r}}'(s) \cdot \bar{\boldsymbol{v}}'(s) = 0 \tag{5}$$

must hold identically. Using Eqs. (1) and (2), we rewrite (3) by introducing tangent and velocity vectors, respectively, according to

$$\boldsymbol{t}(s,t) := \boldsymbol{r}_s(s,t), \tag{6a}$$

$$\boldsymbol{v}(s,t) := \boldsymbol{r}_t(s,t), \tag{6b}$$

which yields the system

$$\boldsymbol{t}_t = \boldsymbol{v}_s, \tag{7a}$$

$$\mu \boldsymbol{v}_t = (N\boldsymbol{t})_s + \mu \boldsymbol{g}. \tag{7b}$$

As the quantity N in (7a) and (7b) is itself unknown, this system has to be augmented by (1), i.e.

$$0 = (\boldsymbol{t}\cdot\boldsymbol{t})_s, \tag{7c}$$

which of course is an algebraic rather than a differential equation.

Combining the quantities (6a) and (6b) and N into a single variable $\boldsymbol{w}$, we may have that Eqs. (7a)–(7c) take the (formal) structure of a *conservation law*,

$$\mathbf{M}\,\boldsymbol{w}_t = [\boldsymbol{F}(\boldsymbol{w})]_s + \boldsymbol{b} =: \mathbf{A}(\boldsymbol{w})\,\boldsymbol{w}_s + \boldsymbol{b}, \tag{8}$$

where $\boldsymbol{t}$, $\boldsymbol{v}$, $\boldsymbol{g}$ are identified with their coordinate triples with respect to the orthonormal basis $\boldsymbol{i}$, $\boldsymbol{j}$, $\boldsymbol{k}$ (cf. Fig. 4), and

$$\boldsymbol{w} = \begin{bmatrix} \boldsymbol{t} \\ \boldsymbol{v} \\ N \end{bmatrix}, \qquad \mathbf{M} = \begin{bmatrix} \mathbf{E} & \mathbf{O} & 0 \\ \mathbf{O} & \mu\mathbf{E} & 0 \\ \mathbf{0}^{\mathrm{T}} & \mathbf{0}^{\mathrm{T}} & 0 \end{bmatrix}, \qquad \mathbf{A}(\boldsymbol{w}) = \begin{bmatrix} \mathbf{O} & \mathbf{E} & \boldsymbol{0} \\ N\mathbf{E} & \mathbf{O} & \boldsymbol{t} \\ \boldsymbol{t}^{\mathrm{T}} & \boldsymbol{0}^{\mathrm{T}} & 0 \end{bmatrix}, \qquad \boldsymbol{b} = \begin{bmatrix} \boldsymbol{0} \\ \mu\boldsymbol{g} \\ 0 \end{bmatrix},$$

here $\mathbf{E}$ denotes the identity matrix. Due to (7c) the mass matrix $\mathbf{M}$ clearly is singular. According to [6], a curve implicitly defined by $z(s,t) = 0$ is called *characteristic* for (8) if $\det[z_t\mathbf{M} - z_s\mathbf{A}(\boldsymbol{w})] = 0$; from the latter condition, we obtain the differential equations $z_s = 0$ and $\mu z_t^2 - N z_s^2 = 0$, respectively. The first equation yields characteristic curves which are parallel to the s-axis in a (t,s)-plane. These curves will not concern us further because they simply incorporate the axial inextensibility corresponding to the kinematic constraint (7c). On the other hand, characteristic curves arising from the second equation may be written as $s = s_c(t)$, thus $z(s,t) = s - s_c(t)$ and consequently

$$\dot{s}_c = \left(\frac{N(s_c,t)}{\mu}\right)^{1/2} \quad \text{or} \quad \dot{s}_c = -\left(\frac{N(s_c,t)}{\mu}\right)^{1/2}. \tag{9}$$

For the string pendulum discussed in Section 1, relations (9) have been integrated utilizing the numerical solution for N; individual results are depicted in Fig. 5b . As indicated by Fig. 5a, the spatial maxima (for φ) of the propagating waves seem to closely follow the calculated characteristic curves. In the next section, we shall show that this observation holds true in great generality, at least as far as our perturbation analysis extends.

In passing, we note that the conservation law (8) is *hyperbolic* only if $N > 0$ [6]; there are no (real) characteristic curves for points with negative tension. Finally, we point out that due to symmetry, the solutions of the eigenvalue equation $\det[\lambda\mathbf{M} - \mathbf{A}(\boldsymbol{w})] = (\mu\lambda^2 - N)^2 = 0$ come up in pairs: there is no distinguished direction orthogonal to the string's tangent. We deduce from (1) that $\boldsymbol{t}\cdot\mathrm{d}\boldsymbol{t} = 0$; consequently, all partial derivatives of $\boldsymbol{t}$ are orthogonal to the string's configuration. More formally, $\boldsymbol{t}_s = \kappa\,\boldsymbol{t}_1^{\perp}$ and $\boldsymbol{t}_t = \omega\,\boldsymbol{t}_2^{\perp}$, with $\boldsymbol{t}_{1,2}^{\perp}$ denoting unit vectors orthogonal to $\boldsymbol{t}$, and $\omega(s,t)$ and $\kappa(s,t)$ being, respectively, the angular velocity of $\boldsymbol{t}$ and the curvature at the point s; by virtue of (7a), clearly $\boldsymbol{v}_s = \boldsymbol{t}_t = \omega\,\boldsymbol{t}_2^{\perp}$ (see Fig. 4).

Near any individual point on the string, we therefore observe a purely transversal motion which is neatly described by the rotation of the tangent vector. In an inextensible string, only transversal waves can propagate with finite velocity. This last statement should be compared to the extensible case where typically longitudinal waves can (and will) occur.

Considering the quantities $\boldsymbol{t}$ and N the most interesting, we may eliminate $\boldsymbol{v}$ from (7a) and (7b) by differentiation, and thus obtain

$$\mu\boldsymbol{t}_{tt} - N\boldsymbol{t}_{ss} = N_{ss}\boldsymbol{t} + 2N_s\boldsymbol{t}_s. \tag{10}$$

Since the second order differential of $\boldsymbol{t}$ satisfies $\boldsymbol{t}\cdot\mathrm{d}^2\boldsymbol{t} = -\mathrm{d}\boldsymbol{t}\cdot\mathrm{d}\boldsymbol{t}$, we have $\boldsymbol{t}\cdot\boldsymbol{t}_{tt} = -\omega^2$ as well as $\boldsymbol{t}\cdot\boldsymbol{t}_{ss} = -\kappa^2$. Projecting (10) onto the tangential direction therefore yields

$$N_{ss} = -\mu\omega^2 + N\kappa^2. \tag{11}$$

It is a remarkable feature of the latter equation that it contains no derivatives of N with respect to t: the further dynamics of the string does not depend on the temporal evolution of the tension. Given the dynamical state of the

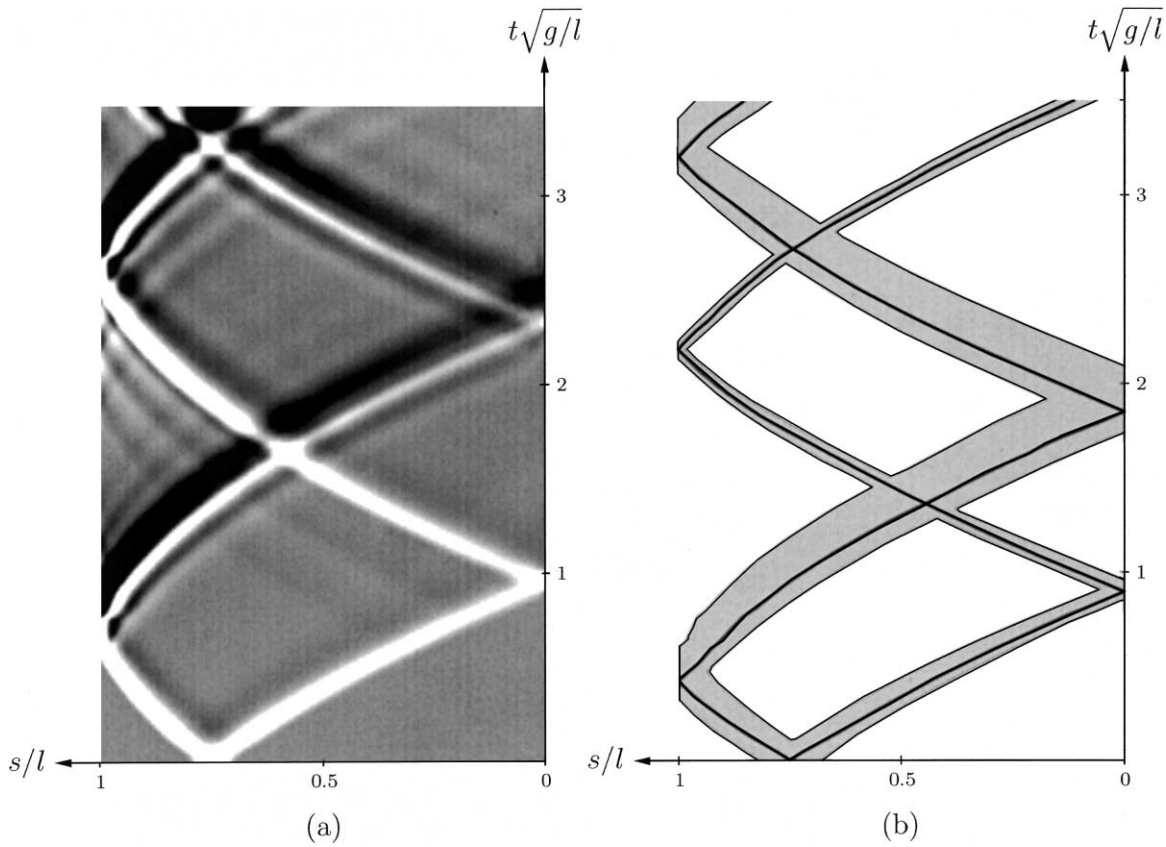

Fig. 5. Top view of Fig. 2 (a) compared to the characteristics starting in $s_c(0) = \frac{3}{4}l$ (b). The gray domain is bounded by the characteristics $s_c(0) = \frac{3}{4}l \pm \frac{1}{15}l$.

string at time t, the tension at that time may be calculated from (11) which by then is just an ordinary differential equation. Especially, the tension in the initial state follows from the initial conditions (4),

$$N_{ss}(s,0) - \bar{\kappa}^2(s)N(s,0) = -\mu\bar{\omega}^2(s), \tag{12}$$

where $\bar{\kappa}^2(s) = |\bar{\boldsymbol{r}}''(s)|^2$ and $\bar{\omega}^2(s) = |\bar{\boldsymbol{v}}'(s)|^2$. We conclude from these observations that any longitudinal information is instantaneously transmitted to every point of the string; there cannot exist a finite velocity of propagation of longitudinal waves.

In case of a planar motion, the equations of motion can be given a more convenient form. Denoting by $\boldsymbol{i}, \boldsymbol{k}$ an orthonormal basis of an inertial frame, we write $\boldsymbol{t}(s,t) = \boldsymbol{i}\sin\varphi(s,t) + \boldsymbol{k}\cos\varphi(s,t)$. Here φ simply measures the angle between $\boldsymbol{k}$ and $\boldsymbol{t}$. Since we have $\mathrm{d}\boldsymbol{t} = \boldsymbol{t}^{\perp}\,\mathrm{d}\varphi$ and $\mathrm{d}^2\boldsymbol{t} = \boldsymbol{t}^{\perp}\,\mathrm{d}^2\varphi - \boldsymbol{t}\,\mathrm{d}\varphi \otimes \mathrm{d}\varphi$ for the first and second order differentials, respectively, (10) may be rewritten as

$$\mu\varphi_{tt}\boldsymbol{t}^{\perp} - \mu\varphi_t^2\boldsymbol{t} - \varphi_{ss}\boldsymbol{t}^{\perp} + N\varphi_s^2\boldsymbol{t} = N_{ss}\boldsymbol{t} + 2N_s\varphi_s\boldsymbol{t}^{\perp},$$

where $\boldsymbol{t}^{\perp}(s,t) := \boldsymbol{i}\cos\varphi(s,t) - \boldsymbol{k}\sin\varphi(s,t)$. Projecting the latter equation onto the local longitudinal and transversal direction, respectively, yields

$$-\mu\varphi_t^2 + N\varphi_s^2 = N_{ss}, \tag{13a}$$

$$\mu\varphi_{tt} - N\varphi_{ss} = 2N_s\varphi_s. \tag{13b}$$

Eq. (13b) constitutes a wave equation for φ describing the propagation of transversal waves. Eq. (13a) which we consider a relation determining the tension N clearly is a copy of (11). By analogously projecting (4), the initial conditions for (13a) and (13b) take the form

$$\varphi(s,0) = \bar{\varphi}(s) := \arccos(\bar{\boldsymbol{r}}'(s)\cdot\boldsymbol{k}) \quad \text{and} \quad \varphi_t(s,0) = \bar{\omega}(s) := \bar{\boldsymbol{v}}'(s)\cdot(\boldsymbol{i}\cos\bar{\varphi}(s) - \boldsymbol{k}\sin\bar{\varphi}(s)). \tag{14}$$

Of course, the initial values of N have to satisfy the compatibility condition (12) with $\bar{\kappa} = \bar{\varphi}'$.

3. Propagation of small transversal waves

A straightforward calculation shows that the only *stationary* solutions (i.e. those not depending on t) of (3) and (10) are given by planar catenary curves [1]. In light of the string pendulum problem sketched in Section 1, we content ourselves with the special case $\boldsymbol{t}(s,t) = \boldsymbol{t}_0 = \text{const.}$ and consequently $N_{ss}(s,t) = 0$, thereby postponing the more general situation to further investigations. Here we thus regard the straight configuration $\boldsymbol{t}_0 = \boldsymbol{k}$ (or, equivalently, $\varphi_0 \equiv 0$) with $N_0(s) = c_0 - d_0 s$ as the reference state of a perturbation analysis. More specifically, we consider the effect of the small planar perturbations $\varphi(s,0) = \bar{\varphi}(s) = \epsilon\bar{\varphi}_1(s)$, $\varphi_t(s,0) = \bar{\omega}(s) = \epsilon\bar{\omega}_1(s)$ with $\epsilon > 0$ denoting a small parameter. Taking as an ansatz the asymptotic expansion [5]

$$N(s,t) = N_0(s) + \sum_{i=1}^{n}\epsilon^i N_i(s,t) + \mathrm{O}(\epsilon^{n+1}), \qquad \varphi(s,t) = \sum_{i=1}^{n}\epsilon^i\varphi_i(s,t) + \mathrm{O}(\epsilon^{n+1}), \tag{15}$$

inserting it into (13a) and collecting powers of ϵ, we obtain

$$\sum_{i=1}^{n}\epsilon^i N_{i,ss} = \sum_{i=1}^{n}\epsilon^{i+1}\left(N_0\sum_{k=1}^{i}\varphi_{k,s}\varphi_{i-k+1,s} + \epsilon\sum_{k=1}^{i}N_k\sum_{l=1}^{i-k+1}\varphi_{l,s}\varphi_{i-k-l+2,s}\right) - \mu\sum_{i=1}^{n}\epsilon^{i+1}\sum_{k=1}^{i}\varphi_{k,t}\varphi_{i-k+1,t} + \mathrm{O}(\epsilon^{n+1})$$

as $\epsilon \to 0$. By balancing powers of ϵ, we arrive at

$$\mathrm{O}(\epsilon): \quad N_{1,ss} = 0, \tag{16a}$$

$$\mathrm{O}(\epsilon^2): \quad N_{2,ss} = N_0\varphi_{1,s}^2 - \mu\varphi_{1,t}^2, \tag{16b}$$

$$\mathrm{O}(\epsilon^i): \quad N_{i,ss} = \sum_{k=1}^{i-1}(N_0\varphi_{k,s}\varphi_{i-k,s} - \mu\varphi_{k,t}\varphi_{i-k,t}) + \sum_{k=1}^{i-2}N_k\sum_{l=1}^{i-k-1}\varphi_{l,s}\varphi_{i-k-l,s} \tag{16c}$$

for $i = 3,\ldots,n$. In an analogous manner, (13b) leads to

$$\mu\sum_{i=1}^{n}\epsilon^i\varphi_{i,tt} - \sum_{i=1}^{n}\epsilon^i\left(N_0\varphi_{i,ss} + \epsilon\sum_{k=1}^{i}N_k\varphi_{i-k+1,ss}\right) = 2\sum_{i=1}^{n}\epsilon^i\left(N_{0,s}\varphi_{i,s} + \sum_{k=1}^{i}N_{k,s}\varphi_{i-k+1,s}\right) + \mathrm{O}(\epsilon^{n+1})$$

as $\epsilon \to 0$; from this we deduce for the individual orders of ϵ

$$\mathrm{O}(\epsilon): \quad \mu\varphi_{1,tt} - N_0\varphi_{1,ss} = 2N_{0,s}\varphi_{1,s}, \tag{17a}$$

$$\mathrm{O}(\epsilon^i): \quad \mu\varphi_{i,tt} - N_0\varphi_{i,ss} = 2N_{0,s}\varphi_{i,s} + \sum_{k=1}^{i-1}(2N_{k,s}\varphi_{i-k,s} + N_k\varphi_{i-k,ss}) \tag{17b}$$

for $i = 2, \ldots, n$. By means of (15), the initial conditions (14) take the form

$$\sum_{i=1}^{n} \epsilon^i \varphi_i(s,0) + \mathrm{O}(\epsilon^{n+1}) = \epsilon \bar{\varphi}_1(s), \tag{18a}$$

$$\sum_{i=1}^{n} \epsilon^i \varphi_{i,t}(s,0) + \mathrm{O}(\epsilon^{n+1}) = \epsilon \bar{\omega}_1(s). \tag{18b}$$

Equating coefficients of ϵ^1 gives the initial conditions corresponding to (17a)

$$\mathrm{O}(\epsilon): \quad \varphi_1(s,0) = \bar{\varphi}_1(s) \quad \text{and} \quad \varphi_{1,t}(s,0) = \bar{\omega}_1(s). \tag{19a}$$

Since $N_0(s) = c_0 - d_0 s$ is already known, φ_1 may be calculated from (17a), and in turn N_2 follows from integrating (16b) twice. But then φ_2 is the only unknown quantity in (17b) with $i = 2$, and the procedure may be repeated. By consequently inserting into (16c) and (17b), each term in the expansion (15) may be determined. By virtue of (18a) and (18b), all the equations (17b) have to be solved under homogenous initial conditions

$$\mathrm{O}(\epsilon^i): \quad \varphi_i(s,0) = 0 \quad \text{and} \quad \varphi_{i,t}(s,0) = 0 \tag{19b}$$

imposed for $i = 2, \ldots, n$. Contrary to (17a), the dynamics of φ_i for $i = 2, \ldots, n$ is exclusively due to a forcing term e_i, which only depends on quantities calculated earlier,

$$\mu \varphi_{i,tt} - (c_0 - d_0 s)\varphi_{i,ss} = -2 d_0 \varphi_{i,s} + e_i, \tag{20}$$

and clearly $e_1 = 0$.

3.1. Representation of solutions

The differential equations (17a) and (20) only differ by their inhomogeneity. Furthermore, they all are of the same type, which is determined by the tension in the unperturbed equilibrium. If $N_0(s) = c_0 - d_0 s < 0$, these equations are elliptic, implying that there is no wave propagation at all. In the sequel, we shall thus assume that $c_0 - d_0 s > 0$. If $d_0 > 0$, then equations (20) are hyperbolic on $s \in (-\infty, c_0/d_0)$. Without loss of generality we subsequently focus on $d_0 \geq 0$.

The case $d_0 = 0$ is somewhat special, so we deal with it separately. From a physical point of view, this situation may be interpreted as describing a light string with a heavy mass attached to its end. (We shall discuss this topic in more detail when dealing with various boundary conditions in [7].) By scaling time according to $\tau := t(c_0/\mu)^{1/2}$, we obtain from (20):

$$\Phi_{i,\tau\tau} - \Phi_{i,ss} = E_i, \tag{21}$$

a family of wave equations for $\Phi_i(s,\tau) := \varphi_i(s, \tau(\mu/c_0)^{1/2})$, where $E_i(s,\tau) := (1/c_0)\, \mathrm{e}_i(s, \tau(\mu/c_0)^{1/2})$. Taking into account the initial conditions (19a) and (19b),

$$\Phi_1(s,0) = \bar{\varphi}(s) =: \bar{\Phi}_1(s) \quad \text{and} \quad \Phi_{1,\tau}(s,0) = \left(\frac{\mu}{c_0}\right)^{1/2} \bar{\omega}(s) =: \bar{\Omega}_1(s) \tag{22}$$

and $\Phi_i(s,0) = 0$, $\Phi_{i,\tau}(s,0) = 0$ for $i \geq 2$ as well as $E_1 = 0$, we arrive at the well-known solution (attributed to d'Alembert)

$$\Phi_1(s,\tau) = \frac{1}{2}\left\{ \bar{\Phi}_1(s+\tau) + \bar{\Phi}_1(s-\tau) + \int_{s-\tau}^{s+\tau} \bar{\Omega}_1(x)\, \mathrm{d}x \right\}, \tag{23}$$

and for $i \geq 2$ [12],

$$\Phi_i(s,\tau) = \frac{1}{2}\int_0^\tau \int_{s-\tau+y}^{s+\tau-y} E_i(x,y)\,\mathrm{d}x\,\mathrm{d}y. \tag{24}$$

In particular, the choice of $\bar{\Omega}_1(s) = \pm\bar{\Phi}'_1(s)$ as the initial conditions forces Φ_1 to be constant along the straight lines $z(s,\tau) = s \pm \tau - a = 0$, where a denotes an arbitrary number. According to (9) with $N = N_0 = c_0$, these lines are the characteristics of (21).

We now turn towards the case $d_0 > 0$; here d_0/μ is the only quantity of physical relevance (whereas c_0 merely shifts the origin of the coordinate s), and so we scale time by $\tau := t(d_0/\mu)^{1/2}$. Furthermore, the new spatial coordinate $\sigma := c_0/d_0 - s$ equals zero exactly where the tension N_0 vanishes. We thus obtain the transformed equations

$$\Phi_{i,\tau\tau} - \sigma\Phi_{i,\sigma\sigma} = 2\Phi_{i,\sigma} + E_i \quad \text{for } (\sigma,\tau) \in (0,\infty)\times(0,\infty), \tag{25a}$$

where analogously $\Phi_i(\sigma,\tau) := \varphi_i(c_0/d_0 - \sigma, \tau(\mu/d_0)^{1/2})$ as well as $E_i(\sigma,\tau) := (1/d_0)\,\mathrm{e}_i(\sigma - c_0/d_0, \tau(\mu/d_0)^{1/2})$. The initial conditions for $i = 1$ now read

$$\Phi_1(\sigma,0) = \bar{\varphi}_1\left(\frac{c_0}{d_0} - \sigma\right) =: \bar{\Phi}_1(\sigma) \quad \text{and} \quad \Phi_{1,\tau}(\sigma,0) = \left(\frac{\mu}{d_0}\right)^{1/2}\bar{\omega}_1\left(\frac{c_0}{d_0} - \sigma\right) =: \bar{\Omega}_1(\sigma), \tag{25b}$$

while for $i \geq 2$, we have vanishing initial data

$$\Phi_i(\sigma,0) = 0 = \bar{\Phi}_i(\sigma) \quad \text{and} \quad \Phi_{i,\tau}(\sigma,0) = 0 = \bar{\Omega}_i(\sigma). \tag{25c}$$

One could solve all these equations by means of series of Bessel functions of first and second kind, $(1/\sqrt{\sigma})J_1(2\nu\sqrt{\sigma})$ and $(1/\sqrt{\sigma})Y_1(2\nu\sqrt{\sigma})$; as long as no boundary conditions have been specified, the eigenvalues ν remain undetermined. Such an analysis of eigenmodes is in fact a classical topic [4]. Since it does not directly make transparent the properties of propagating waves, we shall, however, not pursue this approach but rather derive an expression for the solutions of (25a) which imitates d'Alembert's representation (23). To this end, we observe that the solutions of

$$z_\tau^2 - \sigma z_\sigma^2 = (z_\tau - \sqrt{\sigma}z_\sigma)(z_\tau + \sqrt{\sigma}z_\sigma) = 0$$

may be written as $z(\sigma,\tau) = 2\sqrt{\sigma} \pm \tau - 2\sqrt{A}$ with A denoting a positive number. The characteristics of (25a), implicitly given by $z(\sigma,\tau) = 0$, are easily seen to be parabolas in the (σ,τ)-plane parametrized by τ, they may be written as

$$\sigma = \sigma_0(\tau) = \tfrac{1}{4}(2\sqrt{A} \mp \tau)^2, \tag{26}$$

which simply is the solution of (9) with $N = N_0 = d_0\sigma$ (Fig. 6) . By setting $x := 2\sqrt{\sigma}$ and $y := \tau$ as well as $u_i(x,y) := \Phi_i(\frac{1}{4}x^2, y)$, the set of equations (25a) is transformed to the so-called *second normal form* [12]:

$$u_{i,yy} - u_{i,xx} - \frac{3}{x}u_{i,x} = E_i\left(\frac{1}{4}x^2, y\right) \quad \text{for } (x,y) \in (0,\infty)\times(0,\infty). \tag{27}$$

The characteristics of (27) are given by straight lines in the (x,y)-plane. We shall now discuss (27) by means of a Riemann function. To this end, we observe that the adjoint differential operator of $L[u] := u_{yy} - u_{xx} - (3/x)u_x$ is given by $M[v] := v_{yy} - v_{xx} + (3/x)v_x$, more formally

$$vL[u] - uM[v] = \left((vu)_x - \left(2v_x - \frac{3}{x}v\right)u\right)_x - ((vu)_y - 2v_y u)_y =: \mathrm{rot}(K,J). \tag{28}$$

Integrating the latter relation over the triangle $D = [\mathrm{MPQ}]$ formed by characteristics (cf. Fig. 7) , we find by virtue of Green's theorem

$$\int\int_D (vL[u] - uM[v])\,\mathrm{d}x\,\mathrm{d}y = \int_{\mathrm{M}}^{\mathrm{P}} (K\,\mathrm{d}x + J\,\mathrm{d}y) + \int_{\mathrm{P}}^{\mathrm{Q}} K\,\mathrm{d}x + \int_{\mathrm{Q}}^{\mathrm{M}} (K\,\mathrm{d}x + J\,\mathrm{d}y).$$

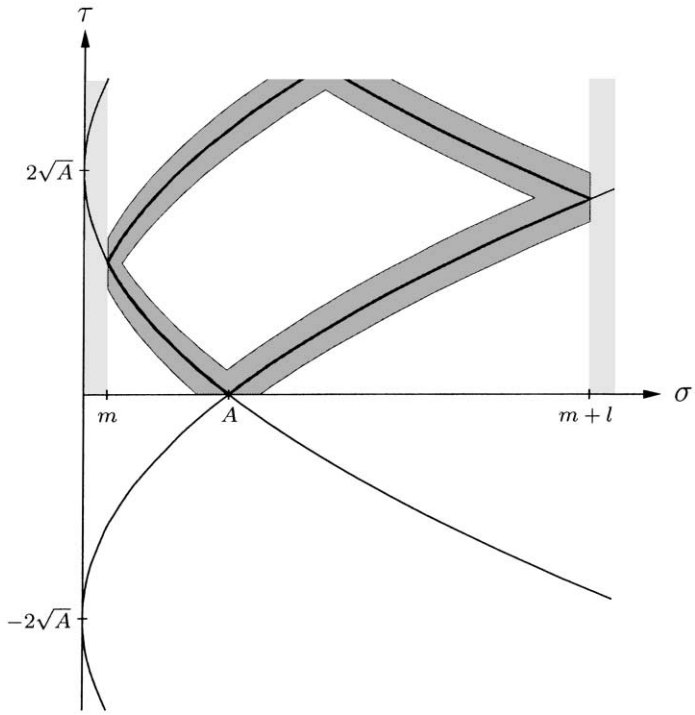

Fig. 6. Characteristics of the equilibrium configuration.

Fixing parameters ξ, η with $\xi > \eta$, we define the function $v = v(x, y; \xi, \eta)$ as the unique solution of the boundary value problem

$$v_{yy} - v_{xx} + \left(\frac{3}{x}v\right)_x = 0 \quad \text{on} \quad D = [\mathrm{MPQ}], \tag{29a}$$

$$v = \left(\frac{x}{\xi}\right)^{3/2} \quad \text{if} \quad (x, y) \in \overline{\mathrm{PM}} \cup \overline{\mathrm{MQ}}. \tag{29b}$$

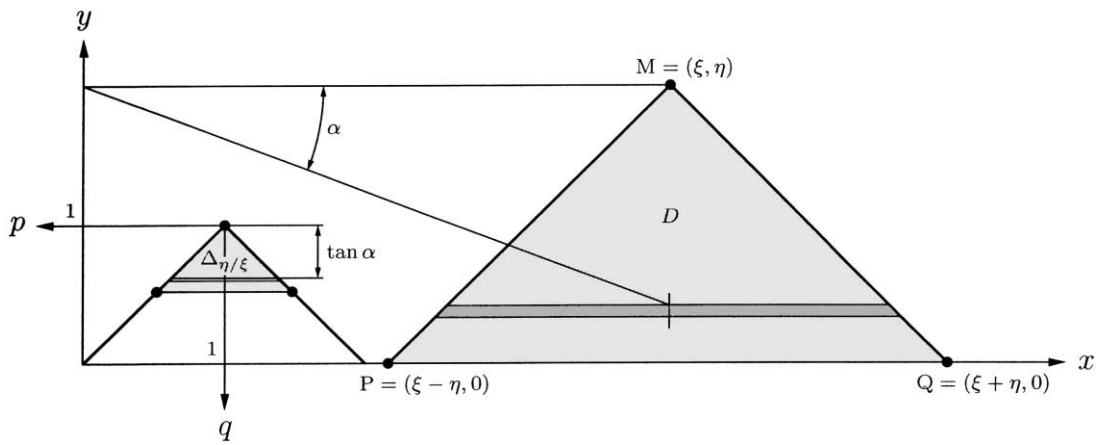

Fig. 7. The domain of integration being transformed to a part of a unit triangle.

Following [12], we call v the *Riemann function* associated with (27). We point out that v is equally referred to as *Green function* throughout the literature; in the light of the forthcoming paper [7], however, we prefer the former notion.

Since $M[v] = 0$, the solution of (27) may be written as

$$u_i(\xi,\eta) = \frac{1}{2}\left\{ u_i(\xi+\eta,0)\, v(\xi+\eta,0;\xi,\eta) + u_i(\xi-\eta,0) v(\xi-\eta,0;\xi,\eta) + \int_{\xi-\eta}^{\xi+\eta} [u_{i,y}(x,0)\, v(x,0;\xi,\eta) - u_i(x,0) v_y(x,0;\xi,\eta)]\,\mathrm{d}x - \int_0^{\eta}\int_{\xi-\eta+y}^{\xi+\eta-y} E_i\left(\frac{1}{4}x^2, y\right) v(x,y;\xi,\eta)\,\mathrm{d}x\,\mathrm{d}y \right\}. \tag{30}$$

From the initial data according to (25b) and (25c) we obtain

$$u_i(x,0) = \bar{\Phi}_i(\tfrac{1}{4}x^2) =: \bar{u}_i(x) \quad \text{and} \quad u_{i,y}(x,0) = \bar{\Omega}_i(\tfrac{1}{4}x^2) =: \bar{w}_i(x). \tag{31}$$

By means of (30), the solutions $\Phi_i(\sigma,\tau) = u_i(2\sqrt{\sigma},\tau)$ of the original problems (25a)–(25c) may be given the representation we were after. For the first order solution, we find

$$\Phi_1(\sigma,\tau) = \frac{1}{2}\left\{ \bar{\Phi}_1\left(\frac{1}{4}(2\sqrt{\sigma}+\tau)^2\right)\left(\frac{2\sqrt{\sigma}+\tau}{2\sqrt{\sigma}}\right)^{3/2} + \bar{\Phi}_1\left(\frac{1}{4}(2\sqrt{\sigma}-\tau)^2\right)\left(\frac{2\sqrt{\sigma}-\tau}{2\sqrt{\sigma}}\right)^{3/2} + \int_{2\sqrt{\sigma}-\tau}^{2\sqrt{\sigma}+\tau}\left[\bar{\Omega}_1\left(\frac{1}{4}x^2\right) v(x,0;2\sqrt{\sigma},\tau) - \bar{\Phi}_1\left(\frac{1}{4}x^2\right) v_y(x,0;2\sqrt{\sigma},\tau)\right]\mathrm{d}x \right\} \tag{32}$$

whereas due to trivial initial data,

$$\Phi_i(\sigma,\tau) = -\frac{1}{2}\int_0^{\tau}\int_{2\sqrt{\sigma}-\tau+y}^{2\sqrt{\sigma}+\tau-y} E_i\left(\frac{1}{4}x^2, y\right) v(x,y;2\sqrt{\sigma},\tau)\,\mathrm{d}x\,\mathrm{d}y \quad \text{for } i = 2,\ldots,n.$$

One should compare the latter formulas to (23): in case of constant N_0 the Riemann function corresponding to (21) identically equals 1 and thus (23) may be considered as an analog of (32).

By its very definition, the Riemann function also depends on the parameter (ξ,η). Nevertheless, it suffices to solve the boundary value problem (29a) and (29b) once, because the different Riemann functions may be transformed to a standard form. To this end, we shall use the notation $\Delta_\delta := \{(p,q) : 0 < |p| < q < \delta\}$. It is easily seen that (29a) and (29b) can be given the normalized form

$$v^*_{qq} - v^*_{pp} - \left(\frac{3}{1-p}v^*\right)_p = 0 \quad \text{for } (p,q) \in \Delta_{\eta/\xi} \subset \Delta_1, \tag{33a}$$

$$v^* = (1-p)^{3/2} \quad \text{if } p = \pm q \tag{33b}$$

by means of the transformation of coordinates $(p,q) := ((\xi-x)/\xi, (\eta-y)/\xi)$, where, accordingly, $v^*(p,q) := v(\xi(1-p), \eta-\xi q; \xi,\eta)$. As suggested by this notation, we shall henceforth consider v^* a function on Δ_1 which does actually not depend on the parameter (cf. Fig. 7). Once v^* is known, the value of v for arbitrary (ξ,η) is given by $v(x,y;\xi,\eta) = v^*((\xi-x)/\xi, (\eta-y)/\xi)$.

The original differential equations (13a) and (13b) subject to the initial conditions (14) has thus been reduced to finding solutions of the boundary value problem (33a) and (33b). Any analytical solution of the latter would clearly give rise to an analytical solution of the former, which we already know to be rather unintuitive. For the purpose of the present calculations, it is much more sensible to use a sufficiently accurate numerical version of the normalized Riemann function v^*.

Let us point out that such a numerical solution may easily be provided. Covering the domain of integration by a grid with width $h = 1/n$ and discretizing (33a) by means of central difference quotients at $(p,q) = (ih, (k+1)h)$,

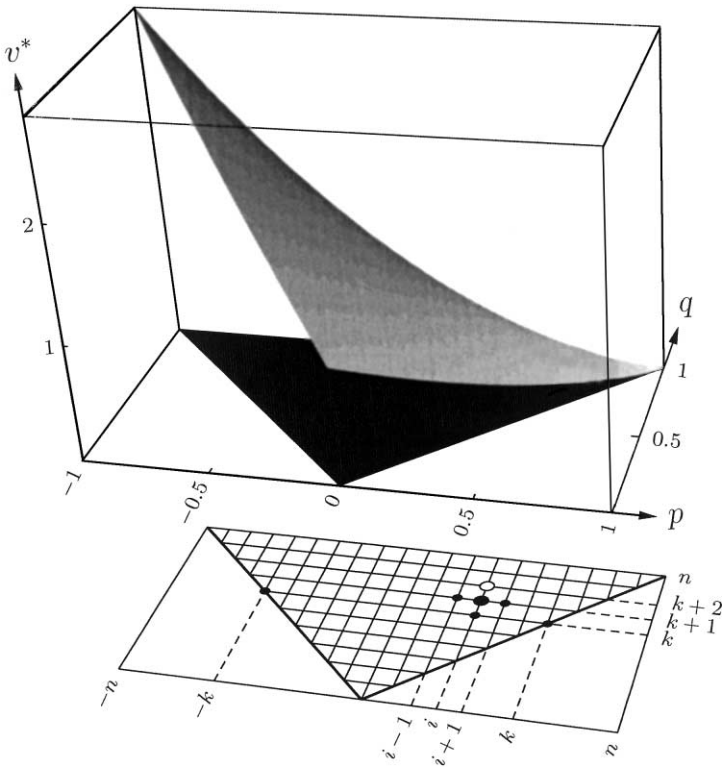

Fig. 8. The normalized Riemann function v^* calculated numerically on a grid with width $h = 1/n$.

we are led to the recursion formula

$$v^*_{i,k+2} = (1 - \tfrac{3}{2}(n - i - 1)^{-1})v^*_{i+1,k+1} + (1 - \tfrac{3}{2}(n - i + 1)^{-1})v^*_{i-1,k+1} - v^*_{i,k}, \tag{34}$$

where $k = 0, \ldots, n$, $i = -k, \ldots, k$ and $v^*_{i,k} := v^*(ih, kh)$. At the boundary $i = \pm k$, we have $v^*_{i,k} = (1 - ih)^{3/2}$. From the recursion formula (34) and the boundary data, the approximate values $v^*_{i,k}$ of the normalized Riemann function may be calculated for every second point of the grid (see Fig. 8).

3.2. First order approximation

It has been mentioned before that the characteristics are all the same for the differential equations (20) coming from the perturbation analysis. These characteristics follow from the static solution $N_0 = c_0 - d_0 s = d_0\sigma$. However, they must not be regarded as the characteristics of the original problem (13a) and (13b) which are obtained from the ordinary differential equations (9) by means of (15). Due to (16a) the tension is linear also on first order, i.e. $N_1(s, t) = c_1(t) - d_1(t)s$ for which we write $N_1(\sigma, \tau) = d_0(C_1(\tau) + D_1(\tau)\sigma)$ with respect to the transformed coordinates σ and τ. Expanding (9), we then obtain

$$\pm\dot{\sigma}_c = \sqrt{\sigma_c} + \frac{C_1(\tau) + D_1(\tau)\sigma_c}{2\sqrt{\sigma_c}}\epsilon + \mathrm{O}(\epsilon^2) \tag{35}$$

as $\epsilon \to 0$. In order to compare the characteristics of the static problem, i.e. (26), to those of the full problem, we also write the latter in form of an asymptotic expansion, i.e. $\sigma_c(\tau) = \sigma_0(\tau) + \sigma_1(\tau)\epsilon + \mathrm{O}(\epsilon^2)$. Equating powers of

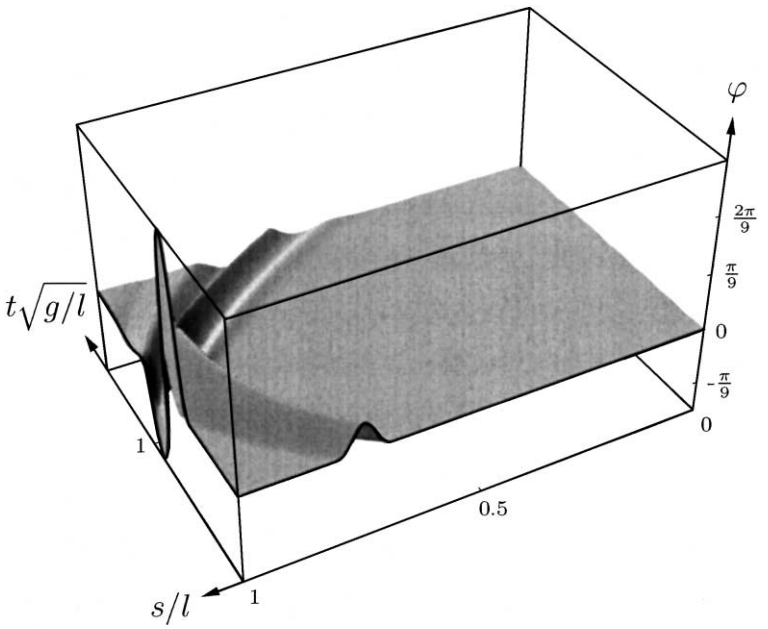

Fig. 9. The evolution of φ due to a small perturbation according to the special initial condition (38).

ϵ, we rediscover on order O(1) the parabolas (26). However, there is a first order correction term given by [1]

$$\sigma_1(\tau) = \pm \int_0^\tau \frac{2\sqrt{A} \pm \tau}{(2\sqrt{A} \pm y)^2} \left[C_1(y) + \frac{1}{4} D_1(y)(2\sqrt{A} \pm y)^2 \right] \mathrm{d}y. \tag{36}$$

Recall that in the case of constant tension the specific choice of initial conditions $\bar{\Omega}_1 = \pm\bar{\Phi}_1'$ made the integral in (23) disappear. One could therefore try to analogously make the corresponding terms vanish in (30) or (32). More precisely, one could tentatively set $\bar{w}_1(x) = \pm\bar{u}_1'(x)$ in (30) or equivalently $\bar{\Omega}_1(\sigma) = \pm\sqrt{\sigma}\bar{\Phi}_1'(\sigma)$ in (30). According to (35) characteristics differ from $\dot{\sigma}_c = \pm\sqrt{\sigma_c}$ already on first order. As a consequence, we merely find

$$u_1(\xi, \eta) = \bar{u}_1(\xi \pm \eta, 0)\, v^*\left(\pm\frac{\eta}{\xi}, \frac{\eta}{\xi}\right) \pm \frac{1}{2}\int_{\xi-\eta}^{\xi+\eta} \bar{u}_1(x) \left[v_p^*\left(1 - \frac{x}{\xi}, \frac{\eta}{\xi}\right) \pm v_q^*\left(1 - \frac{x}{\xi}, \frac{\eta}{\xi}\right)\right] \frac{\mathrm{d}x}{\xi} \tag{37}$$

here. Not only does the integral term (considerably) contribute to u_1 for large η, but there is a certain effect for small η too: From (33b) it is easily seen that $v_p^*(0,0) \pm v_q^*(0,0) = -\frac{3}{2}$ and therefore the integral term behaves like $-(3/\xi)\bar{u}_1(\xi)\eta + \mathrm{O}(\eta^2)$ as $\eta \to 0$. Neglecting the integral in (37) may thus be justified for small η if the initial velocity is chosen according to

$$\pm\bar{w}_1(x) = \bar{u}_1'(x) + \frac{3}{2x}\bar{u}_1(x) \quad \text{or} \quad \pm\bar{\Omega}_1(\sigma) = \sqrt{\sigma}\bar{\Phi}_1'(\sigma) + \frac{3}{4\sqrt{\sigma}}\bar{\Phi}_1(\sigma). \tag{38}$$

In this special case, the first term on the right-hand side of (37) remains unchanged while the integrand vanishes at $\eta = 0$. Going back to the original coordinates $\sigma = \frac{1}{4}x^2$ and $\tau = \eta$, we thus find

$$\Phi_1(\sigma, \tau) = \bar{\Phi}_1\left(\frac{1}{4}(2\sqrt{\sigma} \pm \tau)^2\right)\left(\frac{2\sqrt{\sigma} \pm \tau}{2\sqrt{\sigma}}\right)^{3/2} + \mathrm{O}(\tau^2).$$

[1] Here and in the sequel, equations containing $\pm$ (or $\mp$) should be read as two individual equations exclusively containing the upper or lower signs, respectively.

Along the characteristic (26), the latter relation simply reads

$$\Phi_1(\sigma_0(\tau),\tau) = \bar{\Phi}_1(A)\left(\frac{2\sqrt{A}}{2\sqrt{A}\mp\tau}\right)^{3/2} + \mathrm{O}(\tau^2). \tag{39}$$

As can be seen from Fig. 9, the approximations outlined above agree quite well with the numerical solutions of the full problem. Especially, the initial conditions (38) give rise to nearly "clean" waves propagating in one direction.

4. Conclusions

Wave propagation in inextensible strings results from (locally) purely transversal motions and is completely determined by the rotation of the local tangents (cf. Fig. 4). The characteristic velocity (9) solely depends upon the local value of the tension N. Due to inextensibility, N may be calculated from the tangents' motion alone: at any fixed time it obeys the ordinary differential equation (11).

A string pendulum subject to homogenous gravitation g not only provides a simple example for the methods discussed in the present work but also is suited for practical experiments. For the vertical equilibrium, the tension is easily seen to be $N_0(s) = (m + l - s)\mu g$. (Here the arc-length s is measured from the point of suspension; the quantities l, $l\mu$ and $m\mu$ denote the string's length, its total mass, and the mass attached at the string's end, respectively.) According to (26), the characteristics passing through $s = a$ at $t = 0$ are given by the parabolas

$$s_0(t) = m + l - \frac{1}{4}(2\sqrt{m+l-a} \mp t\sqrt{g})^2. \tag{40}$$

When slightly perturbing this equilibrium state by changing the angles and angular velocities of the local tangents to $\varphi(s,0) = \epsilon\bar{\varphi}_1(s)$ and $\varphi_t(s,0) = \epsilon\bar{\omega}_1(s)$, respectively, the characteristics diverge from (40) even on first order (of ϵ). Nevertheless, by means of (38), it turns out that the special choice of initial conditions

$$\mp\bar{\omega}(s) = \sqrt{g(m+l-s)}\bar{\varphi}'(s) + \frac{3g}{4\sqrt{g(m+l-s)}}\bar{\varphi}(s) \tag{41}$$

gives rise to waves wandering almost exclusively towards the endmass (minus sign) and the point of suspension (plus sign), respectively. As a consequence of (39), initially

$$\varphi(s_0(t),t) \approx \varphi(a,0)\left(\frac{2\sqrt{m+l-a}}{2\sqrt{m+l-a}\mp t\sqrt{g}}\right)^{3/2} \tag{42}$$

holds. Having an eye on d'Alembert's solution of the classical wave equation with constant coefficients, one could possibly have guessed the first term on the right-hand side of (41); the corresponding velocity follows from the characteristic equation $\mu\dot{s}_0^2(0) = N_0(a) = (m+l-a)\mu g$. The second term in (41) however is not revealed without a thorough discussion of the representation (32).

Summarizing we may thus say that by (42) characteristics of the reference state may be interpreted as paths of small local perturbations. These characteristics are quite accurately traced by small waves even after reflections (see Fig. 5 and [7]). We regard this observation as retrospectively giving support to our perturbation analysis. After all, an important feature of (17a) and (17b) is the sole emergence of characteristics of the reference state. As a consequence of (36), the characteristics (9) of the full problem diverge from the latter even on first order and seemingly admit no evident physical interpretation in the present context.

According to (42), a wave travelling towards a region of higher tension accelerates as $|\ddot{s}_0(t)| = \frac{1}{2}g$, thereby shrinking in amplitude like $(1 + \text{const.}\, t)^{-3/2}$. Conversely, waves travelling towards regions of lower tension slow down and simultaneously become bigger according to $(1 - \text{const.}\, t)^{-3/2}$. A physical interpretation of this behavior might be as follows: Since the slope of characteristics increases with increasing tension, the distance between

characteristics grows towards the fixed end and shrinks towards the free end. Assuming an energy-like quantity to be conserved, travelling waves plausibly have to decrease (increase) in amplitude because they are supported on growing (shrinking) domains.

The exponent $\frac{3}{2}$ in (42)) originates from the affine statical tension profile. As indicated by (16a) an affine law may hold for the tension even on higher orders. This fact is quite well confirmed by numerical simulations (see Fig. 3): Following a short period of fluctuations due to the splitting of the initial configuration, the statical tension profile may be found with high accuracy between the two propagating waves. This clear period however is drastically terminated as soon as the free end is reached by the perturbation wave: Oscillations and even shock-like structures in the tension profile can be observed (see Fig. 3). When looking at Figs. 2 and 3, several questions concerning the reflection of propagating waves naturally arise. After all, Fig. 2 suggests that the reflected waves are considerably distorted. A careful discussion of these issues will be accomplished in [7]: There the purely uni-directional waves (42) are going to prove very helpful because they show the reflection of a single wave in a lucid manner (see Fig. 9).

References

[1] S.S. Antman, Nonlinear Problems of Elasticity, Springer, New York, 1995.
[2] V.V. Beletsky, E.M. Levin, Dynamics of Space Tether Systems, American Astronautical Society, Univelt, San Diego, CA, 1993.
[3] G. Hamel, Theoretische Mechanik, Springer, Berlin, 1967.
[4] H. Heuser, Gewöhnliche Differentialgleichungen, Teubner, Stuttgart, 1989.
[5] M.H. Holmes, Introduction to Perturbation Methods, Springer, New York, 1995.
[6] M. Renardy, R.C. Rogers, An Introduction to Partial Differential Equations, Vol. 13, Springer, New York, 1993.
[7] M. Schagerl, A. Berger, Reflection of small waves in inextensible strings, in preparation.
[8] M. Schagerl, A. Berger, On the appropriate treatment of singularly perturbed wave equations, Z. Angew. Math. Mech. 81 (2001) S624–S634.
[9] M. Schagerl, W. Steiner, A. Steindl, H. Troger, On the paradox of the free falling folded chain, Acta Mechanica 125 (1997) 155–168.
[10] M. Shearer, The nonlinear interaction of smooth travelling waves in an elastic string, Wave Motion 7 (1985) 169–175.
[11] M. Shearer, The Riemann problem for the planar motion of an elastic string, J. Differ. Equations 61 (1986) 149–163.
[12] A.N. Tychonov, A.A. Samarski, Partial Differential Equations in Mathematical Physics, Vol. 1, Holden-Day, San Francisco, CA 1967.